

Direct Observation of the 2D Gain Profile in High Power Tapered Semiconductor Optical Amplifiers

Rebecca B. Swertfeger¹, James A. Beil¹, Stephen M. Misak¹, Jeremy Thomas², Jenna Campbell², Daniel Renner², Milan Mashanovitch² and Paul O. Leisher^{1,2,*}

¹Rose-Hulman Institute of Technology, 5500 Wabash Ave, Terre Haute, Indiana, U.S.A.

²Freedom Photonics, LLC., 41 Aero Camino, Santa Barbara, California, U.S.A.

Keywords: Semiconductor Laser, Diode Laser, Semiconductor Amplifier, Tapered Amplifier, Master-Oscillator Power-Amplifier (MOPA), High Power, Beam Quality, Single-Mode, Gain Profile, Longitudinal Spatial Hole Burning, Optical Communication Sources, Free-Space Optical Communication, InGaAsP, InP.

Abstract: A novel experimental approach to permit direct observation of the 2D gain profile in high power tapered semiconductor optical amplifiers and integrated MOPA devices is reported. A two-dimensional simulation of the photon, carrier, and gain distributions inside the tapered amplifier demonstrate gain saturation effects that could be measured by directly viewing the spontaneous emission profile inside of the cavity. Tapered lasers with a built-in window on the back of the device are fabricated and a SWIR microscope camera is used to measure the spontaneous emission profile under operation at varying injection levels. The effect of gain saturation due to stimulated emission is clearly observed and in close agreement with the theoretical model.

1 INTRODUCTION

Modest (watt-class) power levels and diffraction-limited beam quality are required for a variety of diode laser applications including optical communication, narrow linewidth seeding, and pumping. Conventional ridge waveguide lasers are not capable of achieving these output levels due to the low cross-sectional area (high series resistance) and catastrophic optical mirror damage (in devices operating at wavelengths below 1100 nm). For optical communication applications, devices operating around 1500 nm are particularly important. Tapered diode laser master oscillator power amplifier (MOPA) devices grown on InP substrates have shown promise as a source of watt-class diffraction limited optical power at 1550 nm (Donnelly, 1998) and (Selmic, 2002).

The general concept of the tapered MOPA device is as follows. Single-mode laser oscillation occurs within the etched ridge waveguide laser region. Optical power from this single-mode laser section is then output into the mode expansion region, where the fundamental Gaussian beam is free to expand due to diffraction. A flared, or tapered, contact is patterned in this region with an angle that is matched

to the natural diffraction angle of the injected beam. This section operates above saturation intensity and serves to efficiently amplify the signal. Because the beam is free to expand, the cross-sectional area of the device grows with position, keeping the peak intensity much lower than would occur in a traditional high power single-mode ridge waveguide laser (promoting good reliability) and also greatly reducing the thermal resistance of the device, allowing for much higher power extraction than would be possible in a traditional single-mode device. A schematic drawing is shown in Figure 1.

In an ideal taper, the output optical mode from the ridge region propagates along the length of the taper, expanding (due to diffraction) to form a larger version of the same mode. The mode is amplified as the tapered region is pumped with electrical current, leading to high optical output powers. For a fixed taper angle, the longer the taper, the more the mode is expanded and the higher the achievable output power.

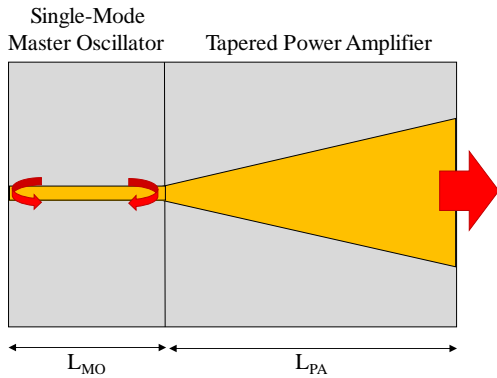


Figure 1: Schematic diagram of a single spatial mode tapered master oscillator (MO) power amplifier (PA) laser.

In real tapered lasers, this ability to scale power while maintaining single-mode performance is limited by the stability of the lateral optical mode. The onset of beam filamentation occurs in regions where the gain is not well-saturated, such as along the edges of the optical mode where the intensity is lower. Reflection at the front facet creates a backwards-travelling wave that can seed laser oscillation, especially in the regions where the carrier density is high due to poor gain clamping.

Because tapered amplifiers are edge-emitting devices, typical measurement techniques do not permit observation of the gain profile (though the integrated amplified spontaneous emission can be measured). In larger laser systems (solid state, fiber, and gas lasers, for example), the gain can be measured through the observation of the spontaneous emission from the side of the laser cavity. High power tapered semiconductor lasers, however, are bonded junction down, and the excess solder that pools along the edge of the device prevents investigation of the gain from the side of the device. Thus, there exists a need for a technique which allows for measurement of the gain profile within the tapered amplifier, and the demonstration of any such approach would greatly benefit the development of tapered laser diodes.

In this paper, a method which permits direct observation of the two-dimensional spontaneous emission profile, and hence gain profile, within a tapered optical amplifier is demonstrated. In the next section, a model which accounts for coupling of the photon density to the gain profile is developed. The subsequent sections report the design of the device and experimental results of the approach.

2 THEORY

2.1 Model Development

Modeling of the 2D photon and carrier distribution in the tapered power amplifier was based on the semiconductor laser rate equations and leveraged our groups' prior work modeling the effects of longitudinal spatial hole burning in broad area semiconductor lasers (Hao, 2014). The standard semiconductor rate equations are modified to permit variation of the local carrier density $N(z)$, local photon density $N_p(z)$, and local gain $g(z)$ with longitudinal position z , as described in equations (1) through (3). In a perfect optical amplifier, feedback from the emitting facet (and cavity resonance) is suppressed, thus it is only necessary to track the forward propagating photon density.

$$\frac{dN(z)}{dt} = \frac{\eta_i I}{qV} - \frac{N(z)}{\tau} - v_g g(z) [N_p(z)] \quad (1)$$

$$\frac{dN_p(z)}{dz} = (\Gamma g(z) - \alpha_i) N_p(z) \quad (2)$$

$$g(z) = g_0 \ln \left(\frac{N(z)}{N_{tr}} \right) \quad (3)$$

The following parameters are defined as follows. η_i is the internal quantum efficiency, I is the injection current, and q is the electron charge. V is the volume of the active region, v_g is the photons' group velocity, Γ is the optical mode confinement factor, α_i is the intrinsic optical loss, g_0 is the gain coefficient, and N_{tr} is the transparency carrier density. τ is the carrier lifetime which includes Auger recombination, Shockley-Read-Hall recombination, and spontaneous radiative recombination (Chuang, 1995).

$$\tau = \frac{1}{A + BN(z) + CN(z)^2} \quad (4)$$

The finite difference method was used to solve the simultaneous differential equations along the length of the cavity. The length of the cavity was divided into 50 steps and once the photon density was known for the first point, it was calculated for the second, and so on. This propagation process was repeated for many steps in the width of the cavity so that a two-dimensional model could be created.

Coupling of the photon population to the carrier population results in an inverse relationship between gain and photon density. Thus, as the injected signal from the master oscillator is amplified along the z -direction of the amplifier, gain and carrier density are

necessarily reduced. Spontaneous emission, which is proportional to the square of carrier density, is used to extract the gain profile.

The two-dimensional distribution of gain is calculated following a quasi 1D approach. Fraunhofer far-field diffraction of the injected optical mode is assumed, resulting in a linear divergence of the fundamental Gaussian-like mode along the cavity length. The diffraction angle is calculated from a 2D cross-sectional effective index simulation of the optical mode in the ridge waveguide of the master oscillator and the unconfined slab which comprises the power amplifier. The total input photons and beam width are used as inputs to the amplifier simulation. At each position z , the local photon and carrier population distributions are computed. As the simulation proceeds to the next segment, the beam is propagated forward and reshaped to follow the calculated diffraction angle. This process is repeated to propagate the beam through the entire length of the amplifier and results in a solved 2D profile of photon density, carrier density, and gain.

2.2 Simulation Results

A tapered optical amplifier operating at 1550 nm was simulated subject to the following parameters: taper length = 2.5 mm, taper angle = 4° , master oscillator ridge width 4.0 μm , tapered amplifier injection current $I_{\text{PA}} = 4000$ mA, and input power supplied from the master oscillator $P_{\text{MO}} = 23$ μW . Additional simulation parameters are reported in (Hao, 2014). Figure 2 depicts the simulated 2D photon density profile in the tapered amplifier section of the device. As shown, the low optical power injected from the master oscillator leads to small signal amplification along the first ~65% of the total length of the amplifier. Gain saturation and linear amplification take over at this point, increasing the total optical power to above 500 mW.

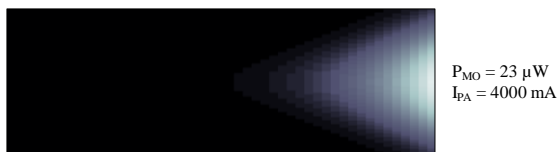


Figure 2: Simulated 2D photon density profile for the tapered MOPA device.

Figure 3 depicts the simulated 2D gain distribution in the tapered amplifier for the case of zero input optical power (amplified spontaneous emission is not included in the model) and for the case of 23 μW input optical power. In the case of zero injected optical power, the 2D gain profile is uniform along the width and length of the taper. The amplification

of the 23 μW signal injected by the master oscillator leads to saturation of the gain in the same region where the photon density is highest, demonstrating the coupling between these two critical parameters.

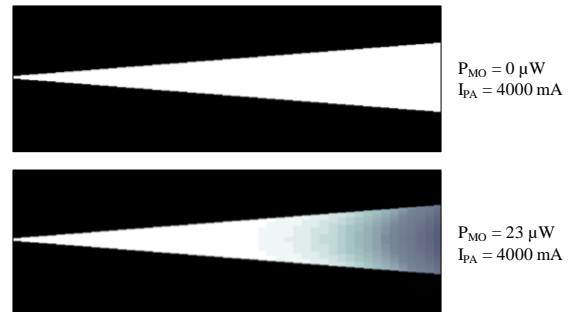


Figure 3: Simulated 2D gain profile for a tapered MOPA device. The asymmetry of the optical photon density leads to gain reduction due to saturation near the front of the amplifier.

3 EXPERIMENT

3.1 Device Design and Fabrication

The integrated master oscillator and tapered power amplifier (MOPA) laser was designed in a manner to permit direct observation of the 2D spontaneous emission profile in the cavity. Figure 4 depicts a basic schematic drawing of the device geometry. The edge-emitting tapered MOPA structure is designed to be soldered junction-down to an expansion-matched heatsink, with separate isolated contacts permitting individual injection of the master oscillator and power amplifier sections. A window opening is patterned on the back (n-side) of the diode to permit viewing of the spontaneous emission from the quantum well along the entire length of the device through a microscope.

The InGaAsP-based semiconductor epitaxial structure was grown by metalorganic chemical vapor deposition (MOCVD) on InP. The InGaAsP waveguide is 500 nm thick with InP used for the cladding layers. The active region comprises two 6.5 nm InGaAsP quantum wells emitting at 1550 nm surrounded by 10 nm InGaAsP barriers. The tapered MOPA devices were fabricated using standard fabrication processes. The single-mode ridge waveguide master oscillator section is designed for a lateral width of 4 μm and was dry etched using chlorine-based reactive ion etching followed by a wet etch clean-up.

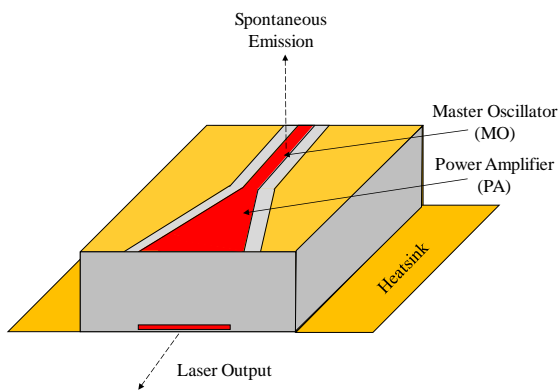


Figure 4: Schematic drawing of the tapered n-window device.

Current confinement is provided through openings lithographically patterned in a SiO_2 insulating layer. The taper angle of 4° corresponds to the full-width $1/e$ divergence angle of the lateral beam in the amplifier section. Laser bars were cleaved to a total length of 4 mm and anti-reflectance coatings were deposited on the rear and front facets, respectively. Feedback at the rear of the master oscillator section is provided by a narrow trench which was etched into the waveguide to permit $\sim 30\%$ reflectance in the waveguide despite the anti-reflectance coating along the back of the device. The devices were hard soldered using AuSn to junction-down to patterned AlN heatsinks which permit separate injection of the master oscillator and power amplifier sections of the device.

Figure 5 depicts a schematic layout of the photomask used in the device fabrication. The pink region represents the dielectric oxide via and hence pumped active area of the chip. The overlap of the lateral optical mode with the lateral gain profile is improved over standard tapered laser designs through control of the current flow. This technique is motivated by prior work wherein the gain of the tapered laser is pixelated (Salet, 1998) and (Walpole, 2000). The blue region shows the window opening in the backside contact which permits viewing of the spontaneous emission profile. The window is pulled back from the injected region of the device by $75\ \mu\text{m}$. Figure 6 depicts optical microscope images of the top-side and bottom-side of three completed chips prior to device singulation.



Figure 5: Layout of the tapered laser structure showing several photomask levels.

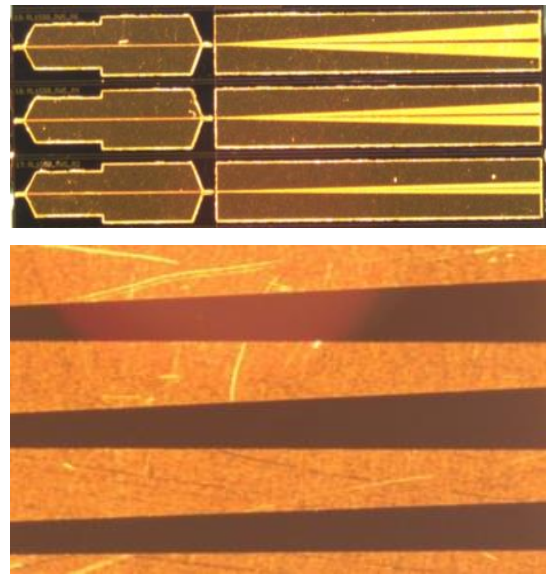


Figure 6: Optical microscope images of the (top) top and (bottom) bottom side of fabricated chips prior to bonding.

3.2 Experimental Setup

A schematic diagram of the experimental setup used to characterize the devices is shown in Figure 7. The shortwave infrared region (SWIR) microscope is configured as follows. A 14-bit WiDy model 640U-S InGaAs camera (640×512 pixel) is mounted to a Navitar near infrared (NIR) zoom system with a 36 mm working distance and capable of 2X to 20X adjustable magnification. Co-axial illumination with a NIR light source is used for initial focusing but turned off for spontaneous emission measurements. The tapered master oscillator power amplifier (MOPA) chip-on-heatsink is attached to a $1\ \text{in}^2$ copper heatsink which is subsequently mounted to a thermoelectric cooling (TEC)-controlled stage. The laser output is collected from the edge of the device by an optical fiber placed near the exit facet, while the spontaneous emission profile can be simultaneously recorded by the camera from the top. For optical power measurements, the fiber is removed from the front of the device and replaced with a thermopile. The current and ridge current are separately controlled and pin probes are used to provide contact to the associated copper contact pads on the alumina heat spreader. Figure 8 depicts a photograph of the experimental setup.

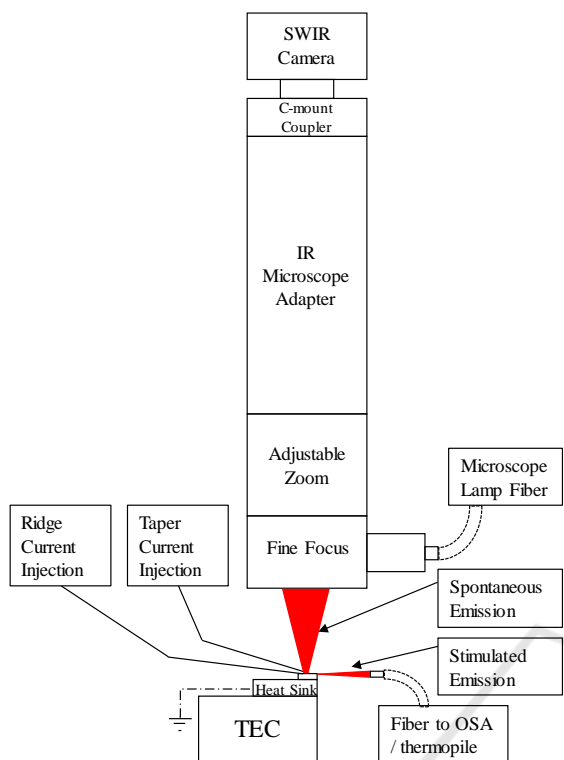


Figure 7: Schematic diagram of the SWIR microscope setup for observation of the 2D spontaneous emission profile.

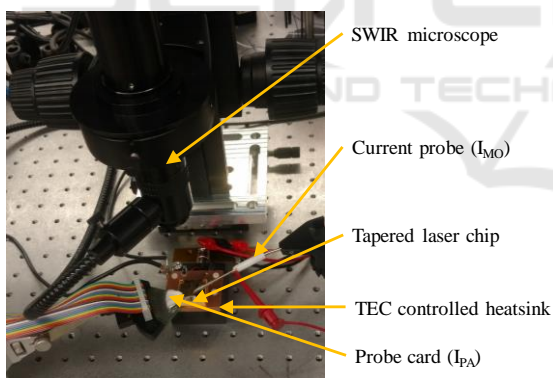


Figure 8: Photograph of the experimental setup.

3.3 Experimental Results

General device characterization of the tapered MOPA structure occurred as follows. All measurements were performed continuous wave at a controlled temperature of 15⁰ C. The device output power was measured as a function of the injected amplifier current for four master oscillator (single-mode ridge section) injection current levels ranging from 0 mA to 300 mA. As shown in Figure 9, a maximum output power of ~400 mW is achieved at $I_{MO} = 300$ mA and $I_{PA} = 4000$ mA. The power vs. current characteristics

clearly shows that the tapered amplifier section does not lase without optical injection from the master oscillator section. The roll/kink behavior observed above 3000 mA is attributed to the onset of multimode oscillation.

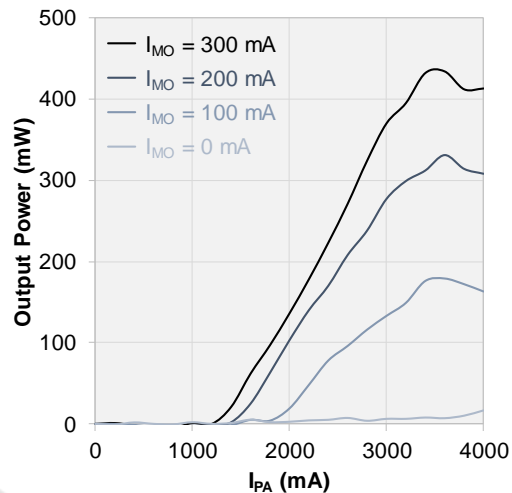


Figure 9: CW power vs. tapered amplifier injection current measured at four master oscillator current values and at a heatsink temperature $T = 15^0$ C.

Figure 10 depicts the measured CW optical spectra for the case where the amplifier current is held constant while the master oscillator injection level is varied. Figure 10 confirms the absence of laser action when the master oscillator is turned off. As the master oscillator current is increased, two features are observed. First, a clear lasing peak appears and red-shifts with increasing IMO. This behavior is attributed to self-heating in the master oscillator section of the device. Second, a large amplified spontaneous emission pedestal appears around the lasing peak. This ASE pedestal occurs due to the excessively high threshold current of the master oscillator section, which lacks any real feedback from the front, and only 30% feedback in the rear. It is clear from this result that the high threshold of the master oscillator section limits the overall efficiency of the device.

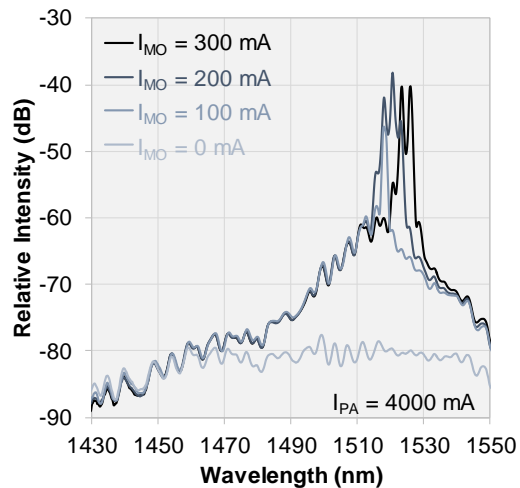


Figure 10: CW optical emission spectrum measured for a constant power amplifier current of 4000 mA at four different master oscillator current values at $T = 15^{\circ}\text{C}$.

Figure 11 depicts the CW optical emission spectra for the case where the master oscillator injection level is held constant while the tapered amplifier current is increased from 1000 mA to 4000 mA. The behavior of this data series lends insight into the operation of the tapered MOPA structure. At a current of 1000 mA, no lasing peak in the amplifier is observed – only the spontaneous emission of the amplifier itself. This is attributed to injection in the amplifier below the transparency current density condition. As the tapered amplifier current increases to 2000 mA, a strong lasing peak at ~ 1500 nm is observed (two longitudinal modes are evident). The background spontaneous emission profile has also increased due to the amplified spontaneous emission in the device. As the current in the tapered amplifier is further increased, the peak lasing wavelength and broadband spontaneous emission profile are red-shifted (again due to self-heating). Less obvious is an apparent reduction in the total amplified spontaneous emission due to increased gain saturation.

Figures 12 and 13 depict the SWIR microscope images taken for the cases where the tapered amplifier current is held constant and where the master oscillator current is held constant, respectively. The apparent blurring of the tapered gain section is not caused by defocus; as previously discussed the current injection is pixelated in this region in order to create a lateral gain profile which better matches the fundamental optical mode amplified in this section. A significant amount of light is seen to scatter off the rear facet of the power amplifier and is caused by the etched trench which serves to provide feedback to the master oscillator.

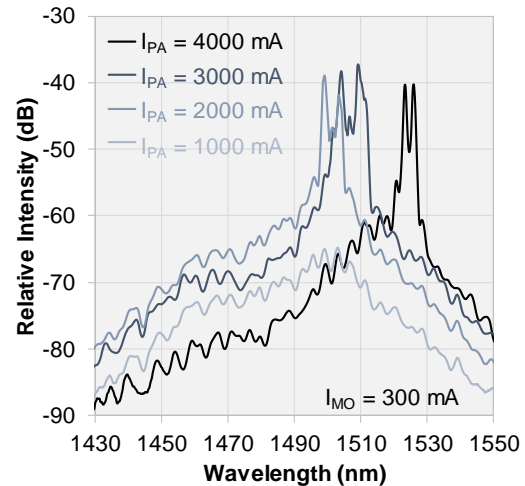


Figure 11: CW optical emission spectrum measured for a constant master oscillator current of 300 mA at four different power amplifier current values at $T = 15^{\circ}\text{C}$.

Scattering of the laser emission can also be seen where the master oscillator and power amplifier intersect and is caused by mode effective index mismatch at this location. A small amount of laser light can be seen scattering at the front facet of the amplifier – this scattered light is attributed to imperfections in the facet cleave or antireflection coating.

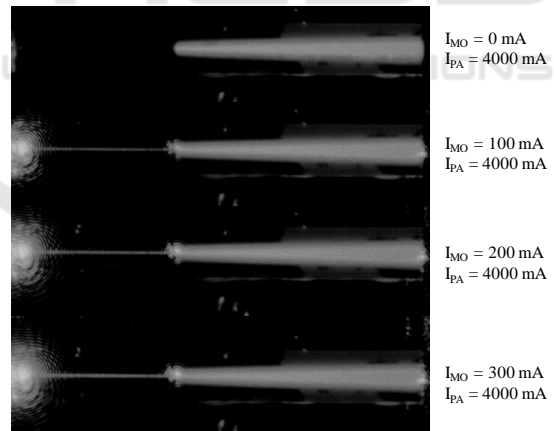


Figure 12: SWIR microscope image of the spontaneous emission measured at a constant tapered amplifier injection current of 4000 mA and varying master oscillator injection current values.

The simulation of this device predicted the low output power of the single-mode master oscillator section would make it difficult to observe the gain saturation effects in the amplifier section. In the analysis of the microscope images taken at $I_{PA} = 4000$ mA, a nonlinear color map was applied in order to investigate the gain saturation effects.

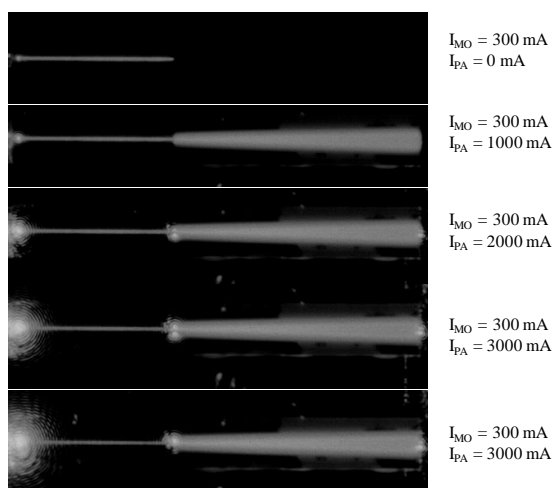


Figure 13: SWIR microscope image of the spontaneous emission measured at a constant master oscillator injection current of 300 mA and varying tapered amplifier injection current values.

Figure 14 depicts the rescaled color map images of the measured spontaneous emission profiles at $I_{MO} = 0$ and 300 mA. As shown, there is a clear decrease in the spontaneous emission, and hence gain, in the final ~35% of the device, just as predicted in the numerical simulations. It is worth noting that the photon density due to stimulated emission is many orders of magnitude higher in this region at 300 mA than at 0 mA. Despite this, a reduction in the light captured by the microscope in this region clearly indicates that the optical signal being measured is spontaneous emission from the quantum well (as opposed to scattered stimulated emission).

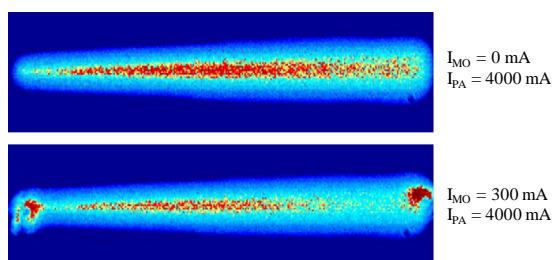


Figure 14: Rescaled color map image comparing the measured spontaneous emission profiles at zero and 300 mA master oscillator injection currents. Suppression of the spontaneous emission near the exit of the facet of the tapered amplifier is a clear indicator of gain reduction due to local saturation.

4 DISCUSSION

The development of high power, high-efficiency tapered amplifiers stands to benefit from measurement techniques which enables a better understanding of the internal device physics. This work, for the first time, enables direct observation of and mapping of the gain saturation effect in a semiconductor optical amplifier. The technique relies on the incorporation of a window in the back-side of the device so that the spontaneous emission profile can be directly observed for devices bonded junction down. This first demonstration utilized a separately addressable tapered MOPA device exhibiting an unusually high master oscillator threshold current attributed to antireflection coatings applied to both sides of the device. Nevertheless, the effects of gain saturation are clearly observed in the images taken. Subsequent work in this area will first focus on applying the technique to devices which operate at much greater output levels. It is expected that this technique will then be used to improve the gain pixelation design to ensure more uniform gain extraction over the entire area of the device.

ACKNOWLEDGEMENTS

The authors acknowledge support by NASA under award number NNX16AD20G.

REFERENCES

- J. P. Donnelly, J. N. Walpole, S. H. Groves, R. J. Bailey, *et al.*, "1.5- μm tapered-gain-region lasers with high-CW output powers," *IEEE Photonics Technology Letters*, vol. 10, pp. 1377-1379, 1998.
- S. R. Selmic, G. A. Evans, T. M. Chou, J. B. Kirk, *et al.*, "Single frequency 1550-nm AlGaInAs-InP tapered high-power laser with a distributed Bragg reflector," *IEEE Photonics Technology Letters*, vol. 14, pp. 890-892, 2002.
- T. Hao, J. Song, and P. O. Leisher, "Rate equation analysis of longitudinal spatial hole burning in high-power semiconductor lasers," *Proc. of SPIE*, pp. 91340S-91340S-7, 2014.
- T. Hao, J. Song, R. Liptak, and P. O. Leisher, "Experimental verification of longitudinal spatial hole burning in high-power diode lasers," *Proc. SPIE*, pp. 90810U-90810U-9, 2014.
- S. L. Chuang, *Physics of optoelectronic devices*. New York: Wiley, 1995.
- P. Salet, F. Gerard, T. Fillion, A. Pinquier, *et al.*, "1.1-W continuous-wave 1480-nm semiconductor lasers with

distributed electrodes for mode shaping," *IEEE Photonics Technology Letters*, vol. 10, pp. 1706-1708, 1998.

J. N. Walpole, J. P. Donnelly, L. J. Missaggia, Z. L. Liao, *et al.*, "Gaussian patterned contacts for improved beam stability of 1.55-um tapered lasers," *Photonics Technology Letters, IEEE*, vol. 12, pp. 257-259, 2000.

